

Konrad-Zuse-Zentrum
für Informationstechnik Berlin

ZIB

Takustraße 7
D-14195 Berlin-Dahlem
Germany

Stefan Zachow, Michael Zilske, Hans-Christian Hege

3D reconstruction of individual anatomy from medical image data: Segmentation and geometry processing

3D reconstruction of individual anatomy from medical image data: Segmentation and geometry processing

Stefan Zachow, Michael Zilske, Hans-Christian Hege

Zuse Institute Berlin (ZIB), Germany

Summary

For medical diagnosis, visualization, and model-based therapy planning three-dimensional geometric reconstructions of individual anatomical structures are often indispensable. Computer-assisted, model-based planning procedures typically cover specific modifications of “virtual anatomy” as well as numeric simulations of associated phenomena, like e.g. mechanical loads, fluid dynamics, or diffusion processes, in order to evaluate a potential therapeutic outcome. Since internal anatomical structures cannot be measured optically or mechanically in vivo, three-dimensional reconstruction of tomographic image data remains the method of choice. In this work the process chain of individual anatomy reconstruction is described which consists of segmentation of medical image data, geometrical reconstruction of all relevant tissue interfaces, up to the generation of geometric approximations (boundary surfaces and volumetric meshes) of three-dimensional anatomy being suited for finite element analysis. All results presented herein are generated with amira[®] – a highly interactive software system for 3D data analysis, visualization and geometry reconstruction.

Keywords

Medical image segmentation, computational geometry, virtual anatomy, finite element meshes

1. “Virtual anatomy” – 3D computer models of individual anatomy

3D geometry models of human anatomy are becoming increasingly relevant in the digital ages. Not only for entertainment or education but also for businesses where human models are involved (e.g. virtual crash tests), or in medicine with respect to patient specific computer assisted therapy planning. Research in the latter field is rapidly advancing. We can distinguish between *generic anatomy* represented by atlases, that demonstrate anatomical structures and their relationships, and *individual anatomy*, that becomes of interest in cases where pathological situations need further attention with respect to any kind of medical treatment. Generic anatomy models can be the result of careful design using modeling software, whereas patient specific anatomy models typically come as an output of an appropriate scanning device, associated with point cloud or image based reconstruction algorithms. However, corresponding sets of individual anatomy models can in turn be combined into generic models using statistical averaging of 3D shapes. Within this work we will focus on the reconstruction of individual anatomy from medical image data for computer assisted treatment planning and numerical simulations.

1.1 Medical imaging yields insight

In order to reconstruct three-dimensional geometry from medical image data appropriate imaging techniques are required. A suitable technique is tomographic imaging (CT, MRI), where a contiguous series of image slices is captured non-invasively. Each slice represents a cut through the scanned structure with a particular thickness. The pixels within each image slice are represented by scalar values that can be interpreted as intensity values (Fig. 1.1). Each intensity value within that pixel matrix is an averaged measurement of material properties at that particular location of the scanned structure. In computed tomography, for instance, the X-ray absorption rate is measured, normalized to the absorption rate of water, given in so-called Hounsfield units. Regions of homogeneous intensity values typically represent anatomical structures, whereas strong gradients are indicators of tissue boundaries. The smallest structures that can be reconstructed from such images depend on the image resolution, i.e. the pixel dimensions. Medical images are typically stored in DICOM format, and dedicated image readers are required for visualization.

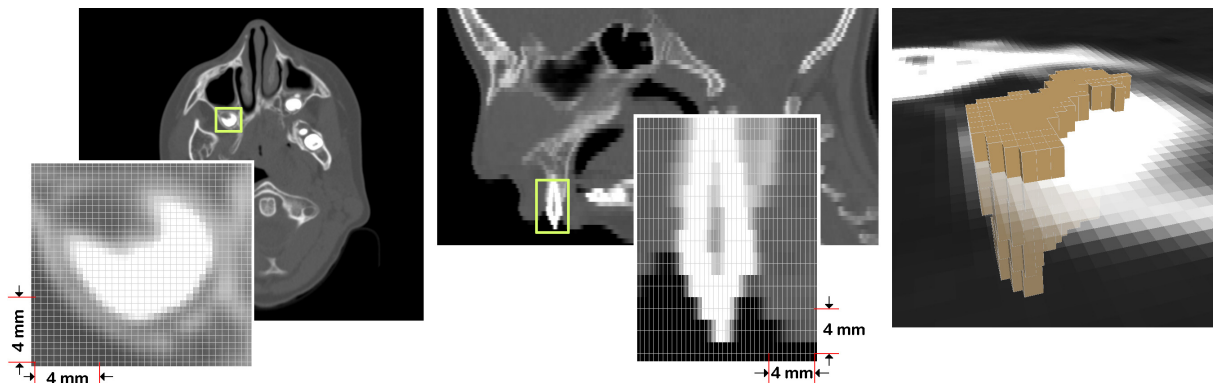


Fig. 1.1: 3D medical image data: From pixels to voxels

Image slices can be concatenated according to the slice position of the respective tomographic measurement, thus forming a three-dimensional image stack (equally or non-uniformly spaced). Anatomical structures of interest can now be traced between adjacent images (Fig. 1.1). Stacking those sliced structures on top of each other reveals an approximation of their three-dimensional shape [1]. The closer the inter-slice distance is, the more accurate will be the spatial reconstruction. Ideally, the distance between consecutive slices equals the pixel resolution. Pulling pixels and slices together we obtain a three-dimensional partition of the image space into volume elements (voxels) forming a 3D scalar field.

Though 3D scalar fields can already be visualized directly using so-called volume rendering techniques [2, 3], such data cannot be modified in an easy way and do not provide a reasonable input for FE simulation (even though finite difference or finite element methods often are applied to labeled voxel data directly due to the lack of suitable geometry reconstruction methods). The major challenge will be to recover the inherent 3D shapes of anatomical structures from 3D medical image data as accurately as possible, and to convert them into geometry. Such structures are described topographically by their boundaries, and these boundaries are implicitly given by means of the classification of voxels, after the entire data volume has been segmented into different regions. Each

voxel gets a particular tissue type assigned. Connected voxels of the same type represent tissue structures (e.g., organs). Structures can again be embedded in other structures, in total forming a complex 3D anatomy model.

2. The amira[®] geometry reconstruction pipeline

With the process of geometry reconstruction we move from 3D voxel space to 2D boundary surfaces embedded in \mathbb{R}^3 , hence extracting information and massively reducing data. The most popular methods do approximate an implicit surface (e.g., via an iso-value) from a 3D scalar field with a polygonal representation [4, 5]. Dividing a 3D scalar field on base of a grey value threshold into foreground and background voxels only works if structures of interest are separable that way. In computed tomography, bone, soft tissue and air can be roughly discriminated by characteristic scalar values. Thus, soft tissue to air interfaces (skin) as well as soft tissue to bone interfaces can be quickly computed as iso-surfaces (i.e. surfaces passing through voxels of the same scalar value). The so-called marching cubes algorithm [4] and its derivatives do reconstruct such implicit surfaces according to this principle using a fast look-up method (Fig. 2.1). As a result, boundary surfaces are represented by a rather large set of piecewise linear surface primitives, i.e. triangles, that are convenient to render since graphics hardware is optimized in this regard.

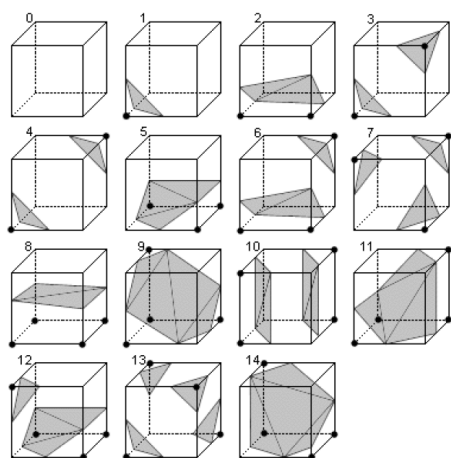


Fig. 2.1: Classical marching cubes look-up for binary classification

Although iso-surfaces are an appealing method for the analysis of 3D scalar fields, they are sensitive to noise and partial volume effects (i.e. voxels that do represent an average value of two or even more adjacent materials), thus introducing speckles or unintended holes. Also in case nested structures or multi-material components have to be reconstructed, standard iso-surface methods are unemployable, since they produce so-called manifold surfaces that do not represent material interfaces in regions where more than two materials are adjacent to each other. This, however, is not an unusual case for anatomical tissue structures and has to be modeled accordingly. In addition, imaging artifacts introduce distortions or lead to erroneous intensity values that prevent any grey-value based method from reconstructing the correct tissue boundaries automatically. Hence, more sophisticated tools and methods are needed for accurate 3D geometry reconstruction.

In the subsequent part of this article we focus on the geometric reconstruction of anatomical structures from three-dimensional medical image data, i.e. the generation of surface and volume meshes in a finite-element sense. At ZIB a dedicated software for medical image processing and geometry reconstruction is being developed, which is called amira[®] [6].¹ Sequences of medical images in DICOM format can be easily imported. The resulting 3D scalar fields can be visualized and inherent structures can be analyzed in many different ways. A commercial version of amira[®] is distributed by Visage Imaging.² Due to a technology transfer agreement between ZIB and VI new methods developed at ZIB become also part of the commercial product, and most of the functionality that is going to be presented is already available therein. Since cutting edge research problems often lead to novel sophisticated methods and to new quality enhancing features, this technology transfer continues and constantly improves the functionality of the commercial version of the software.

2.1 Medical image segmentation

The drawbacks of iso-surface reconstruction have been shortly discussed. Hence, threshold based segmentation might serve as a preprocessing step to any kind of elaborate segmentation strategy. The simplest method would be to correct the segmentation within each image slice using a brush like tool. Surprisingly this is also one of the most commonly used methods in clinical practice. Other tools, such as a *magic wand* for 2D and 3D region growing, *intelligent scissors* for semi-automatic contouring, *deformable contours* that are attracted by image gradients, up to inter-slice interpolation, wrapping, and modification of segmented structures in a 3D view, provide a reasonable support for complex image segmentation tasks. A good example for a large set of such sophisticated selection

¹ <http://amira.zib.de>

² <http://www.visageimaging.com>

tools is provided within the well known image processing software Adobe Photoshop[®]. In its latest version it is also enabled to read images in DICOM format, thus images can be easily converted into region masks that describe anatomical entities within an image slice. Such image masks can be exported to any popular image format, thus being further processed with amira[®] (as long as Adobe does not release some kind of 3D post-processing software for converting stacks of binary region masks into 3D geometry).

The constant use of the software in medical research projects at ZIB with their complex requirements led to practical experience and consequently to the development of features that are quite helpful for medical image segmentation. One is the possibility to mark and classify image areas in any of three orthogonal views with an immediate feed-back in all other views including a three-dimensional visualization (Fig. 2.2). Another is the possibility to assign a multiplicity of materials (in contrast to iso-value segmentation), thus being able to segment a data volume into a multi-material compound. A set of morphological operators such as erosion and dilation (i.e. shrink and grow), as well as smoothing, speckle reduction and consistency tests finally enable a user to create a consistent decomposition of a 3D medical image stack into anatomically meaningful segments. The segmentation result is finally represented in the form of a 3D label field.

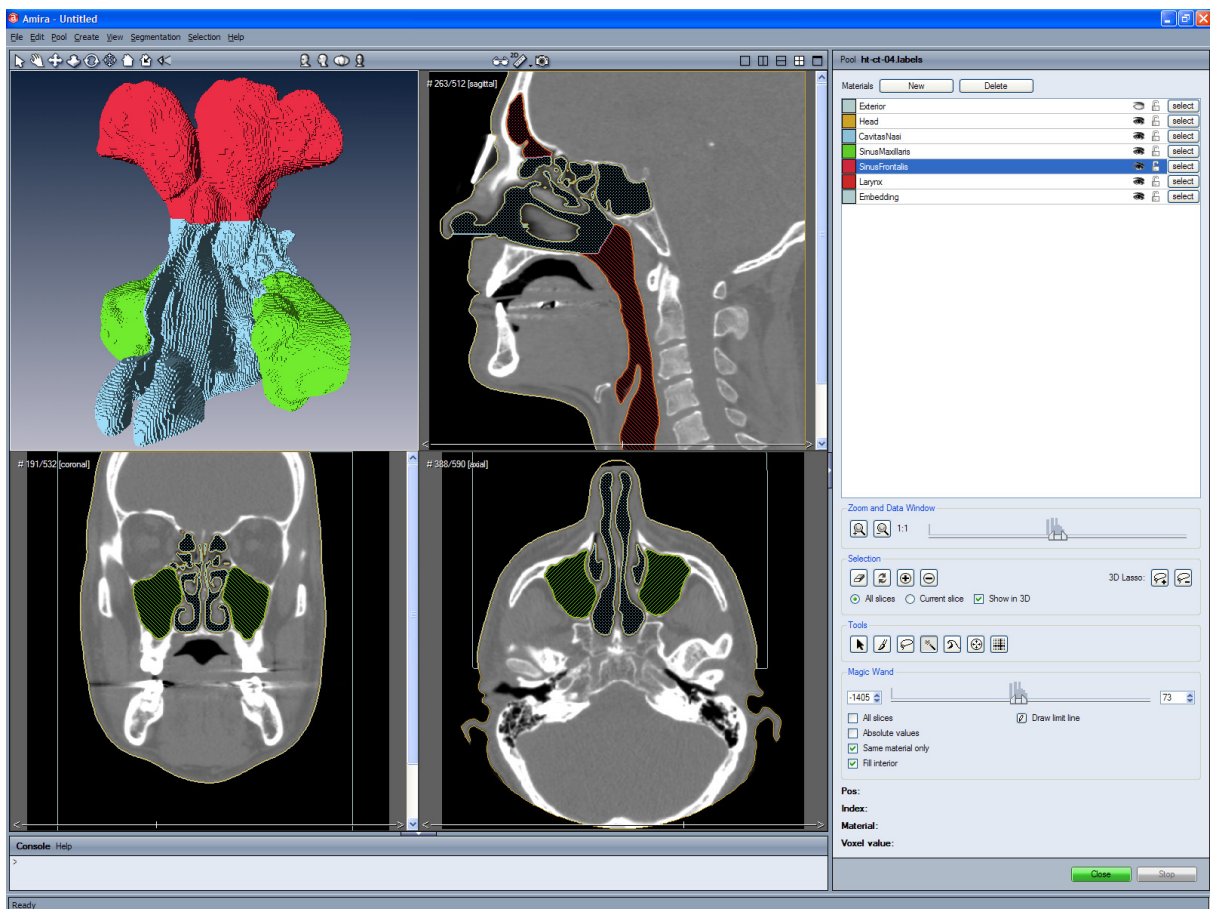


Fig. 2.2: Segmentation editor of amira[®]

With an increasing amount of image slices due to an ever increasing resolution of scanning devices, a manual segmentation approach, however, becomes a less useful option. Since the segmentation process is a rather labor intensive task, current research at ZIB is directed towards a robust and fully automated segmentation of tissue structures [7, 8].

2.2 Boundary surface reconstruction

Typically anatomical structures are of complex shape, normally smooth, and with curved boundary surfaces whose preservation is of importance. *Exterior boundaries* separate structures of interest and background. *Interior boundaries* do separate anatomical regions that have different properties, i.e. contact areas between different tissues. Keeping the complexity of anatomical shapes with all relevant details as well as its multi-material nature, and generating consistent boundary surfaces is our primary

objective. In practice, curved boundaries are often approximated by piecewise linear boundaries. With respect to the reconstruction of arbitrary details, triangulations are the most flexible approach. Though other surface representations are conceivable, we will focus on surface triangulations due to its relevance for computer graphics visualization and finite element methods.

From a given 3D scalar field of labeled voxels³ all boundary surfaces are to be computed. A marching cubes type algorithm would process the 3D data in scan-line order and determines triangle vertices using linear interpolation between adjacent slices – using *binary classification* – meaning that the data is supposed to contain only two materials. The standard marching cubes algorithm attempts to locate the surface in a so-called grid cell, created from eight pixels in two adjacent slices, having one pixel corresponding to each vertex in the corners of a cube (see Fig. 2.1). The algorithm determines in which configuration a surface intersects the cube, and then proceeds (marches) to the next grid cell.

In contrast, a segmentation with amira[®] usually leads to 3D label fields consisting of more than two materials. For creating all separating interfaces a new approach based on *non-binary classification* is required. This problem has been addressed by other groups via a tetrahedral decomposition of grid cells based on a so-called marching tetrahedra principle [9, 10]. At ZIB a generalization of the marching cubes method has been developed for a fast and robust generation of boundary surfaces from non-binary data [11]. Surfaces generated that way do not necessarily belong to a single material, but are constructed of patches, separating volumes of two different materials. Grid cells are traversed and classified according to their configuration of material affiliations. The configurations of vertices within a grid cell dictate how the resulting interfaces are divided into different patches (Fig. 2.2). The algorithm can handle up to eight different vertex classes within the same grid cell, i.e. it is possible for up to eight different materials to meet in a single voxel. The resulting approximation of the material boundaries via a polygonal representation is computed by interpolating material affiliations within each voxel of the 3D label field [12].

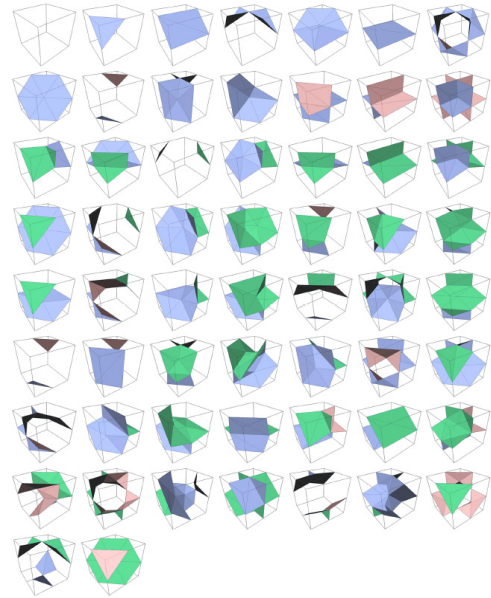


Fig. 2.2: Generalized look-up for up to three different vertex classes

Different smoothing strategies are investigated for the computation of material weights that either preserve previously assigned labels or re-compute them in an appropriate manner to achieve smooth triangulations [13]. In comparison to other existing approaches that may require user interaction to resolve ambiguities, the surface reconstruction method which is implemented in amira[®] is completely automatic, sufficiently fast due to a look-up table approach, and it assures a topological correct solution of the resulting polygonal representation. Two connected regions always share common boundaries, thus, a single triangle always separates two materials, acting as a material interface. However, due to the multi-material nature surface triangulations generated that way might contain *edges* that belong to more than two triangles. Such triangulations are also referred to as non-manifold.

³ in amira[®] a labeled pixel within an image slice represents the center of the voxel surrounding it
Prepared for submission to the 25th CADFEM Users' Meeting 2007

3. "Virtual anatomy" in a finite-element sense

Many physical phenomena in engineering such as mechanical deformation, heat transfer, fluid flow, electromagnetic wave propagation, etc. can be modeled by partial differential equations (PDEs). Such models are also applicable in life sciences where biochemical or biophysical phenomena are to be simulated. The number of possible applications seems to be almost infinite, and we are rather at the beginning of being able to model and simulate really complex matter within living systems. In case PDEs have complicated boundary conditions or are posed on irregularly shaped objects, they usually do not admit closed-form solutions. A numerical approximation of the solution, e.g., using the *finite element method* (FEM) or the *finite volume method* (FVM) is thus necessary. Admittedly, most objects worth simulating do have complicated shapes, and so in general do have anatomical structures. To make them amenable to analysis, they are decomposed into simple shapes, i.e. triangles or quadrilaterals respectively tetrahedrons or hexahedra. A consistent mesh topology and a sufficient mesh quality are vital for an accurate numerical simulation.

Generating FE meshes from CAD models is a well established topic in mechanical engineering. Though in complex cases it often is a challenging task, the effort in geometric modeling is negligible in view of the duration such models are being used in conjunction with numerical simulations, and the value that can be drawn thereof. For individual anatomy, however, things are different. The modeling becomes even more complicated since there are no parametric rules of generation or technical drawings available that can be easily converted into 3D geometry; tomographic imaging is just the only option. Furthermore, geometric models of individual anatomy cannot be reused many times, resulting in an unbalanced situation between modeling effort and benefit, which of course is not guaranteed and has to be proven. Hence, the fast and robust generation of FE meshes for arbitrarily shaped biological structures is a matter of current research in medical engineering and geometry processing [14, 15].

At this point within our geometry reconstruction pipeline we are able to generate accurate boundary surface representations of anatomical structures of interest from 3D medical image data (Fig. 3.1). Surface models that have been generated that way are represented by triangulations whose density depends on the dimensions and the resolution of the underlying 3D scalar field. The dimensions correlate with the size of the structure of interest. The spatial resolution depends on the sampling theory, saying that sampling has to be at least two times higher than the size of the smallest object that is to be captured. Today's conventional tomographic imaging techniques typically yield images with a pixel matrix of 512x512 and a resolution of about 0.5mm/pixel. The minimum distance for the slice reconstruction is about 0.5mm as well, resulting in isometric voxels. This resolution might even double within the next decade. The number of slices depends on the structure that is to be scanned. A full body scan thus leads to 1500 to 2000 images, delivering 3D scalar fields of about 5×10^8 voxels. Since the initial triangulation that is constructed from a segmented data volume occurs on sub-voxel resolution, the number of triangles might amount to several tenths of millions very quickly.

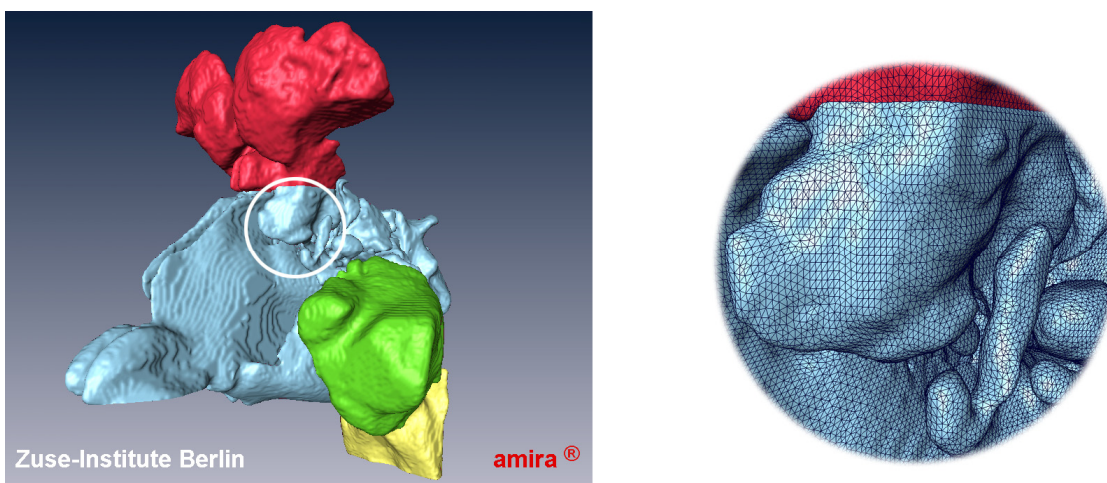


Fig. 3.1: High resolution surface model of the upper respiratory tract (950,000 triangles in total)

The complexity of a numerical simulation depends at least linearly on the number of nodes respectively the number of degrees of freedom within the mesh. Since surface reconstructions from medical image data are considerably over-sampled, a major requirement is the reduction of the high

Prepared for submission to the 25th CADFEM Users' Meeting 2007

resolution via surface simplification. Appropriate algorithms do better adapt sampling to geometry by decreasing the amount of geometric primitives (triangles), while preserving topology, detail and consistency of the surface meshes [16, 17]. The allowable resolution is determined by: i) local curvature that will be approximated by piecewise linear elements, ii) global geometry constraints (i.e. thin structures or narrow regions that have to be approximated by a sufficient number of volume elements inside), and iii) material dependent specifications defined by the modeler. Assuming that all relevant geometric details are captured accurately in a given surface model, its triangulation can be seen as one particular instance of the surface geometry of interest. We aim at generating new instances (e.g., new triangle meshes) of this surface geometry that better fit application specific demands on complexity, sampling, regularity, connectivity, gradation, and quality [18].

3.1 Finite-element surface meshes with amira[®]

In amira[®] a surface simplification algorithm is provided that is based on quadric error metrics [19]. The algorithm uses iterative contractions of vertex pairs to simplify triangulations, while maintaining surface error approximations using quadric matrices, i.e. 4x4 matrices that represent the sum of the squared distances from the respective vertices to the planes of their neighboring triangles. The error that is introduced by a vertex-merge (or edge collapse) operation can be quickly derived from the sum of the quadric error metrics of the vertex pair being merged, and that sum will become the merged vertex's error metric. The algorithm always removes the vertex pair with the lowest error from the top of a priority queue that is constantly updated, and merges it. Quadric error metrics provide a fast and simple way to guide the simplification process with minor memory consumption. Furthermore, the algorithm is not restricted to manifold topology, because disconnected vertices closer than a given threshold may merge as well. This makes it very attractive for non-manifold multi-material surfaces as being generated by amira[®]. An adaptive threshold selection scheme, as well as a fast Fibonacci heap accelerate the simplification process, thus making it applicable even for dense triangulations (Fig. 3.2).

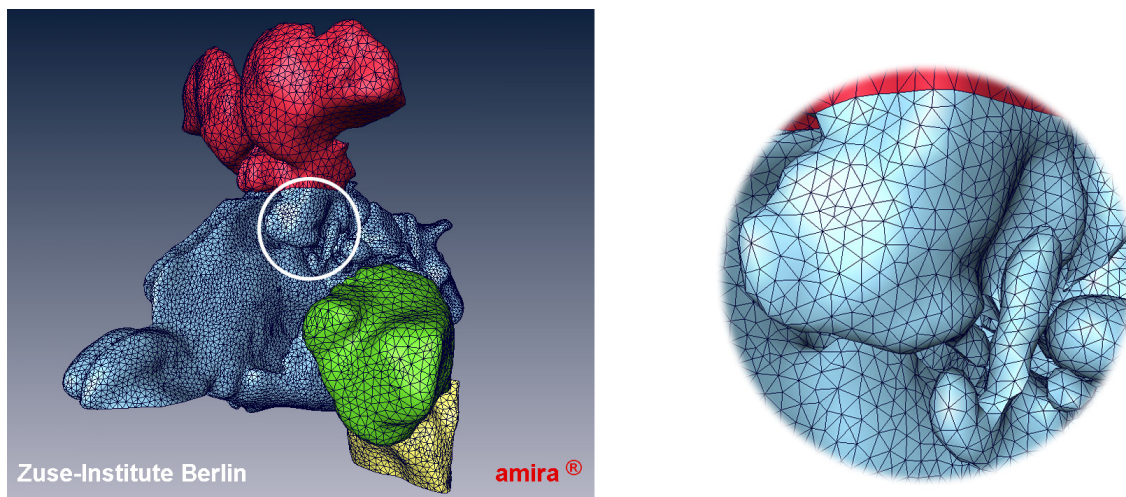


Fig. 3.2: Simplified surface model of the upper respiratory tract (87,000 triangles)

In view of generating volumetric meshes from simplified surface models an additional constraint has to be taken into account. In case non-connected planar boundaries are relatively close together and the space in between is to be filled with elements, the triangle resolution of the respective regions matters. In case it becomes too coarse due to the planarity, only flat tetrahedrons with a bad aspect ratio can be fitted into that space. In order to generate 'good' tetrahedrons [20] resolution has to be adapted locally with respect to the geometrical extents. To this end, an extension of the aforementioned simplification scheme for adaptive point sampling has been developed that takes not only local curvature (i.e. quadric error metrics) into account but also additional mesh density control information. The latter is computed from the distance between non-connected boundaries of the surface model, taking into account that a minimum amount of 'good' tetrahedrons are to be generated between two boundary surfaces. The density field is evaluated during simplification as an additional criterion within the priority queue. That way simplification can be locally controlled by quadric error metrics as well as edge length limitation. Density fields can also be specified by the modeler (either interactively or analytically) with regard to any desired mesh gradation [22, 23].

Even though we are able to drastically reduce the number of triangles while controlling the error that is being introduced within the simplification process, we still have the problem of providing a finite element compatible mesh in the end. Self-intersections might occur as a result of heavy simplification, triangles can become badly shaped with respect to an optimal equilateral triangle, and too small dihedral angles (angles between surface normals of adjacent triangles) prevent a subsequent volumetric meshing step from being able to produce 'really good' elements (i.e. tetrahedrons) [20, 21]. In addition, the larger the rate of the mesh size variation, the worse is the shape quality of the adapted mesh. However, the success of the finite element method depends on the shapes of these tetrahedrons. Large angles within elements cause large interpolation errors as well as discretization errors, thus leading to a less accurate numerical simulation. Small angles, however, might render the stiffness matrices being associated with the finite element method ill-conditioned. Within the commercial version of amira[®] several tools are provided i) to check for situations like this, ii) to correct them in an automated way using a heuristic approach, and in case nothing helps iii) to correct them manually. The latter possibility is especially useful in situations that are algorithmically intractable.

At ZIB a certain effort has been undertaken to improve and to automate the generation of finite element compatible surface triangulations. Especially for therapy planning and simulation in medicine complex multi-material meshes are needed and the amount of time to generate such meshes was to be reduced. In view of generating high quality finite-element meshes automatically, a novel surface simplification and remeshing scheme has been developed. At this stage of the pipeline, the input mesh is taken to be a topologically faithful representation of the modeled geometry. Further modifications, e.g. edge contractions, are restricted to preserve the topological type, taking into account that the mesh may be non-manifold [24]. Vertex positions are always kept on the input surface. After simplification, the sampling is adapted to a user-specified density function, which may take into account the surface curvature and possibly the aforementioned global geometrical constraints. This is accomplished by performing a series of vertex relocations and angle-improving (Delaunay) edge-flips. Vertices are moved within their star, and are mapped back to the input surface using a local parameterization approach. The new position of a vertex is computed as follows: In a first stage, the sampling is adapted by moving vertices so that the areas of its neighboring triangles relate to the given density function. Precise isotropic sample placement is achieved in a second stage, where vertices are moved to coincide with the weighted centroid (with respect to the density function) of their Voronoi cell (Lloyd's relaxation algorithm) [25]. In case a highly regular mesh is desired, vertex valences can also be forced to be six by a series of edge flips. Afterwards the mesh will be polished using angle-based smoothing [26] (Fig. 3.3).

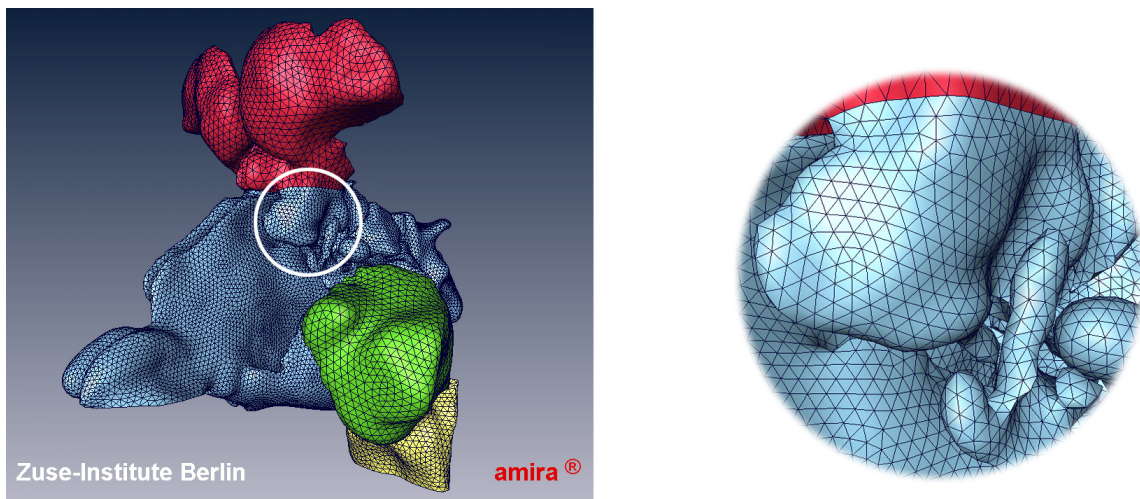


Fig. 3.3: Remeshed surface model of the upper respiratory tract (88,000 triangles)

Non-manifold vertices must be treated separately. Vertices on seams (i.e. patch boundaries) have a neighborhood homeomorphic to one or more than two triangles sharing a common edge. They can only be moved uni-variantly along the seam they reside on. Singular vertices with more complicated neighborhoods remain fixed in their positions. In just the same way as with seams, the remeshing scheme can accommodate feature curves embedded within the input mesh and reproduce them within the output. Thus, sharp geometric features of the input mesh can be preserved, as well as user-defined curves, for example to interactively cut a surface or segment it into patches. Seams and

feature lines are treated in a unified way and are collectively regarded as feature skeleton [27]. To ensure a good triangle quality in the vicinity of a feature skeleton, its sampling must precisely match the sampling of the surrounding mesh. This is accomplished using a novel scheme to dynamically add or remove vertices on the feature skeleton using a connectivity-based criterion, resulting in feature lines and seams which blend nicely into the surrounding mesh.

3.3 Volumetric finite-element meshes

Having a closed triangulation of any structures of interest, either with or without interior boundaries, a conforming volumetric mesh is to be produced that serves as a computational domain for finite-element analysis. The intention in a finite-element sense is to generate a mesh with the *lowest possible* number of elements (where '*lowest possible*' depends on the problem that is to be solved on that grid) in combination with the *highest possible* element quality. Here, it is worth being mentioned that the worst element might be responsible for success or failure of a simulation, thus '*best quality*' cannot be regarded as an average value over all elements [20]. Our boundary triangulations representing all relevant details are already optimized with regard to element quality and size. It is now the task of the volumetric meshing approach to generate an appropriate grid accordingly. Many strategies are conceivable for generating volumetric meshes from a given surface triangulation, depending on whether structured or unstructured meshes are desired, or e.g. Delaunay criteria have to be met [28, 29]. Theoretically, any meshing software can be used. In amira[®] an advancing front approach has been implemented since it is particularly suited for domains with complicated boundaries and internal interfaces [30, 31]. Advancing front techniques belong to the class of heuristic mesh generation methods. The name refers to the strategy of generating elements successively from an ever shrinking set of dynamic surfaces that starts at the boundaries and internal interfaces of the domain and advances into its interior (Fig. 3.4).

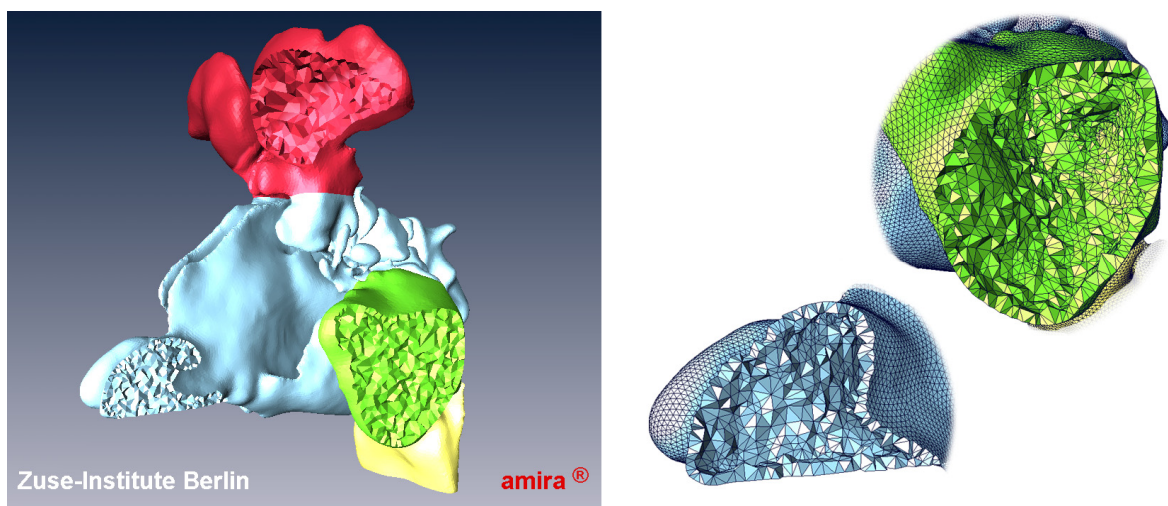
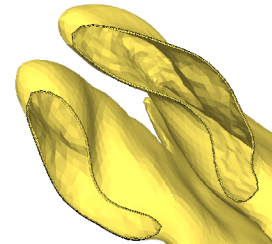


Fig. 3.4: Unstructured volumetric mesh of the upper respiratory tract, right) first front of tetrahedrons

Controlling the size and thus the number of the elements is an important issue. As mentioned before, the intention is to keep the number of elements at a minimum. If elements of uniform size are used throughout the entire mesh, this size will be determined by the most demanding portion of the problem domain in order to guarantee sufficient accuracy (both in geometrical approximation and numerical solution). Consequently, large parts of the mesh might be over-sampled incurring excessively large computational demands. Thus, a mesh generator should offer gradation from small to large element sizes and vice versa. The advancing front principle is well suited for such a demand, since elements are introduced successively, starting with a given resolution that can either be increased or decreased within a certain limit (e.g., by a small percentage of the actual element size). However, this is a rather *blind* method with respect to the global mesh size gradation. Hence, in ZIB projects a global mesh gradation control via a 3D density field is used, which is evaluated during node placement. In case the element size (volume, height, edge length) is coded into the scalar field, a look-up allows for an appropriate node placement according to a global mesh size gradation. The way the density field is constructed depends on the problem that is to be solved. Besides interactive definition by the modeler, appropriate methods are: i) the use of distance fields, ii) scattered data interpolation, or iii) mean value coordinates, for the propagation of the mesh size from the given boundaries into the volume.

At Zuse-Institute Berlin (ZIB) 3D anatomy models are being used in many different applications, such as therapy planning in hyperthermia (electromagnetic wave propagation, temperature distribution), cranio-maxillofacial surgery (soft tissue deformation), orthopedic surgery (biomechanics, hard tissue deformation), functional rhino-surgery (CFD air-flow), electro-cardiology (electrical potentials), and many more.⁴ In all cases the mesh quality is of utmost importance since numerical simulations are always involved. A thorough discussion of mesh quality for various cases certainly is of interest at this point but due to lack of space will be subject of a another publication. For tetrahedral meshes we obtain in general dihedral angles between 6 and 160° with an aspect ratio quality of about 70 – 80% in average. These values can even be improved in case slight modifications of the initial surface geometry will be allowed. Regarding *mixed element type meshes* we are doing the first steps: in CFD projects we are generating wedge-shaped wall elements from tetrahedral grids in order to provide finite-element models for fluid flow simulations with proper wall shear stress analysis. A more extensive support within amira[®] is one of the future directions of development.



4. Conclusions and future work

A geometry reconstruction pipeline from 3D medical image data to finite element meshes of individual anatomical structures has been described as it is provided with amira[®] – a highly interactive software system for 3D data analysis, visualization and geometry reconstruction. It has been shown that even for complex anatomical shapes composed of various materials high quality finite element meshes can be obtained. Rapid prototyping in combination with implantology and prosthetics will foster the convergence of CAD and FE modeling within the medical domain. Numerical simulations might shift the focus away from animal testing to the computer. However, geometry reconstruction from tomographic image data is not restricted to medical applications only. Non-destructive materials testing, geosciences, and paleontology, to name only a few disciplines, also benefit from reverse engineering and modeling techniques as described within this work.

5. References

- [1] Born G: "*Die Plattenmodelliermethode*", Zeitschrift für wissenschaftliche mikroskopische Technik, No. 1, 1884, pp. 278–282
- [2] Hanson CD and CR Johnson: "*The Visualization Handbook*", Academic Press, 2004
- [3] Preim B and D Bartz: "*Visualization in Medicine: Theory, Algorithms, and Applications*", Morgan Kaufman, 2007
- [4] Lorensen WE and HE Cline: "*Marching Cubes: A high resolution 3-D surface construction algorithm*", ACM Siggraph Computer Graphics, Vol. 21, 1987, pp. 163–169
- [5] Bloomenthal J: "*Polygonization of implicit surfaces*", Comp Aid Geom Design, Vol 5, 1988, pp. 341–355
- [6] Stalling D et al.: "*Amira: A Highly Interactive System for Visual Data Analysis*", In [2], chapter 38, 2005, pp. 749–767
- [7] Neubert K et al.: "*Model-based autosegmentation of brain structures in the honeybee using statistical shape models*", excerpt of her bachelor thesis "*Model-based Autosegmentation of Brain Structures in the Honeybee, Apis Mellifera*", Proc. 8th Int. Congr. of Neuroethology, 2007
- [8] Kainmüller D et al.: "*Shape constrained automatic segmentation of the liver based on a heuristic intensity model*", MICCAI Workshop on 3D Segmentation in the Clinic: A Grand Challenge, 2007
- [9] Bloomenthal J and K Ferguson: "*Polygonization of non-manifold implicit surfaces*", ACM Siggraph Computer Graphics, Vol. 29, 1995, pp. 309–316
- [10] Nielson GM and R Franke: "*Computing the separating surface for segmented data*", IEEE Visualization, 1997, pp. 229–233
- [11] Hege HC et al.: "*A generalized marching cubes algorithm based on non-binary classifications*", ZIB Report SC 97-05, 1997
- [12] Stalling D et al.: "*Weighted labels for 3D image segmentation*", ZIB Report SC 98-39, 1998
- [13] Westerhoff M: "*Extracting geometrical models of neuronal structures from 3D image data*", Dissertation, FU Berlin, 2004
- [14] Cezbral JR and R Löhner: "*From medical images to anatomically accurate finite element grids*", Int. Journal For Numerical Methods in Engineering, 51(8), 2001, 985–1008
- [15] Young P et al.: "*Automating the generation of 3D finite element models based on medical imaging data*", Digital Human Modeling for Design and Eng. Conf., 2006, Art. 51
- [16] Heckbert PS and M Garland: "*Survey of polygonal surface simplification algorithms*", ACM Siggraph Computer Graphics, 1997, Course Notes
- [17] Luebke DP. "*A developer's survey of polygonal simplification algorithms*", IEEE Computer Graphics and Applications, 2001, 24–35

⁴ <http://www.zib.de/visual/medical/projects>

- [18] Frey PJ: “*Generation and adaptation of computational surface meshes from discrete anatomical data*”, Int. J. Numer. Meth. Eng., 2004, 1049–1074
- [19] Garland M and PS Heckbert: “*Surface simplification using quadric error metrics*”, ACM Siggraph Computer Graphics, Vol. 31, 1997, pp. 209–216
- [20] Shewchuk JR: “*What is a good linear finite element? Interpolation, conditioning, anisotropy, and quality measures*”, Proc. 11th Int. Meshing Roundtable, 2002, pp. 115–126
- [21] Frey PJ and H Borouchaki: “*Surface mesh quality evaluation*”, Int. J. Numer. Meth. Eng., 1999, 101–118
- [22] Schreiner J et al.: “*Direct (re)meshing for efficient surface processing*”, Proc. Eurographics 25(3), 2006, pp. 527–536
- [23] Borouchaki H et al.: “*Mesh gradation control*”, Int. J. Numer. Meth. Eng., 1998, 1143–1165
- [24] Vivodtzev F et al.: “*Topology preserving simplification of 2D non-manifold meshes with embedded structures*”, The Visual Computer 21, 2005, pp. 679–688
- [25] Surashzky V et al.: “*Isotropic remeshing of surfaces: A local parameterization approach*”, Proc. 12th Int. Meshing Roundtable, 2003, pp. 215–224
- [26] Surashzky V and C Gotsman: “*Explicit surface remeshing*”, Eurographics/ACM Siggraph Symposium on Geometry Processing, 2003, pp. 20–30
- [27] Vorsatz J et al.: “*Dynamic remeshing and applications*”, Proc. 8th ACM symposium on Solid modeling and applications, 2003, pp. 167–175
- [28] George PL: “*Automatic mesh generation: Application to finite element method*”, John Wiley & Sons, 1991
- [29] Owen SJ: “*A survey of unstructured mesh generation technology*”, Proc. 7th Int. Meshing Roundtable, Sandia National Lab., 1998, pp. 239–267
- [30] Lo, SH: “*Automatic mesh generation over intersecting surfaces*”, Int. Journal for Numerical Methods in Engineering 38, pp. 943–954 (1995)
- [31] Rassinoux A: “*Generation and optimization of tetrahedral meshes by advancing front technique*”, Int. J. for Numer. Meth. Eng. 41, 1998, pp. 651–674
- [32] Zachow S et al.: “*CFD Simulation of nasal airflow: Towards treatment planning for functional rhinosurgery*”, Int. J. Comp. Assist. Radiol. Surg., 2006, pp. 165–167